

AD-A025351

RIA-76-U277

Cy No. 2

TECHNICAL LIBRARY

AD-
A025 351
R-CR-76-014



EXPERIMENTATION AND ANALYSIS TO PERFECT A SHOCK PERTURBATION TECHNIQUE

HUGH N. POWELL

FINAL REPORT



PREPARED BY

CONTRACT NO. DAAF 03-71-C-0320

The University of Wisconsin
1500 Johnson Drive
Madison, Wisconsin 53706

Approved for public release, distribution unlimited.

PREPARED FOR

RESEARCH DIRECTORATE
GENERAL THOMAS J. RODMAN LABORATORY
ROCK ISLAND ARSENAL
ROCK ISLAND, ILLINOIS 61201

DISPOSITION INSTRUCTIONS:

Destroy this report when it is no longer needed. Do not return to the originator.

DISCLAIMER:

The findings of this report are not to be construed as an official Department of the Army position unless so designated by other authorized documents.

REPORT DOCUMENTATION PAGE		READ INSTRUCTIONS BEFORE COMPLETING FORM
1. REPORT NUMBER R-CR-76-014	2. GOVT ACCESSION NO.	3. RECIPIENT'S CATALOG NUMBER
4. TITLE (and Subtitle) EXPERIMENTATION AND ANALYSIS TO PERFECT A SHOCK PERTURBATION TECHNIQUE		5. TYPE OF REPORT & PERIOD COVERED Final
		6. PERFORMING ORG. REPORT NUMBER
7. AUTHOR(s) Hugh N. Powell		8. CONTRACT OR GRANT NUMBER(s) DAAF 03-71-C-0320
9. PERFORMING ORGANIZATION NAME AND ADDRESS University of Wisconsin - Madison 1500 Johnson Drive Madison, Wisconsin 53706		10. PROGRAM ELEMENT, PROJECT, TASK AREA & WORK UNIT NUMBERS AMCMS 552D.11.80700.16 DA 1J5622604A607
11. CONTROLLING OFFICE NAME AND ADDRESS Commander, Rock Island Arsenal GEN Thomas J. Rodman Laboratory, SARRI-LR Rock Island, Illinois 61201		12. REPORT DATE April 1976
		13. NUMBER OF PAGES 36
14. MONITORING AGENCY NAME & ADDRESS (if different from Controlling Office)		15. SECURITY CLASS. (of this report) UNCLASSIFIED
		15a. DECLASSIFICATION/DOWNGRADING SCHEDULE
16. DISTRIBUTION STATEMENT (of this Report) Approved for public release; Distribution Unlimited		
17. DISTRIBUTION STATEMENT (of the abstract entered in Block 20, if different from Report)		
18. SUPPLEMENTARY NOTES		
19. KEY WORDS (Continue on reverse side if necessary and identify by block number) Shock Tube Equipment Construction Operation Thermal Conductivity		
20. ABSTRACT (Continue on reverse side if necessary and identify by block number) The overall design of a shock tube has been validated with an extraordinary level of performance. It has been demonstrated that shock Mach numbers up to $M^*=12$ can be predicted to better than $\pm 2\%$ (95% confidence limits) and that the purely aerodynamic losses account for about a 1% decrease in the observed shock Mach numbers relative to the ideal performance values. These results set quite a new level of control for large high performance shock tube installations. The mechanical design work with complete reliability		

is demonstrated after extensive "de-bugging" the combustion, control and test section. The diaphragm rupture and folding system also functions with complete reliability with respect to diaphragm tearing, etc., but a presently unresolved problem is a material failure which occurs after 15 to 20 shots.

FOREWORD

This report was prepared by Prof. Hugh N. Powell of the University of Wisconsin at Madison, Wisconsin under Basic Agreement DAAF 03-71-C-0320, Program Element 62604A, Task Area Number 00, Work Unit Number 029M1.

The contract was part of a propellant gas convective heat transfer study authorized and funded by the U.S. Army Small Arms Systems Agency, DA Project 1W562604A607. The work was conducted under the direction of the Research Directorate, GEN Thomas J. Rodman Laboratory, Rock Island Arsenal, Rock Island, Illinois with Rao Yalamanchili as project engineer.

CONTENTS

	<u>Page</u>
DD Form 1473	i
Foreword	iii
Contents	iv
Introduction	1
Summary of Results	1
(A) Shock Tube Design, Construction and Performance	1
(B) Thermal Conductivity Measurement in High Temperature Gases	2
(C) Other Relevant Information	3
Technical Discussion	4
(A) Summary of Novel Design Features and the Tubes Operation	4
(B) Comparison of Theory and Experiment	9
(C) Range of Accessible Mach Numbers	14
Immediate and Long Range Objectives	15
Contribution of the Army Contract	15
Distribution	S1

INTRODUCTION

The generation of thermochemical properties for any propellant under consideration is essential to the development of a capability to perform overall heat transfer analysis and thereafter stress analysis for any given dimensions of the weapon and for any specified propellant characteristics. As the propellant burns at appropriate burning rates after the initiation of ignition, typical hot propellant gases of the order of 5000°F and 60000 psi will be generated. The transport properties, such as thermal conductivity and viscosity, of various species at high temperatures and high pressures are essential before these properties can be estimated for the mixture under consideration.

I SUMMARY OF RESULTS

(A) Shock Tube Design, Construction and Performance

1. The overall design concept has been validated with an extraordinary level of performance. It has been demonstrated that shock Mach numbers up to $M^* = 12$ can be predicted to better than $\pm 2\%$ (95% confidence limits) and that the purely aerodynamic losses account for about a 1% decrease in the observed shock Mach numbers relative to the ideal performance values. In the writer's opinion, these results set a quite new level of control for large, high performance shock tube installations.

2. After extensive "de-bugging" the combustion, control and test section mechanical design work with complete reliability. The diaphragm rupture and folding system also functions with complete reliability with respect to diaphragm tearing, etc., but a presently unresolved problem is a material failure which occurs after 15 to 20 shots.

3. The electronic shock velocity timing system is about 95% complete. Its completion has been delayed because inadequate funding put us at a disadvantage in completing for electronic technician services.* Slow deliveries of electronic components were also a factor. Until recently similar financial constraints delayed the construction of the entropy wave optical detection system. Now however construction is underway and is currently about 50% complete. This is the last major component needed for thermophysical property measurement.

(B) Thermal Conductivity Measurement in High Temperature Gases

In large measure for the reasons outlined in paragraph (3) above, it has not been possible to actually start using the installation for thermophysical property measurement. While the making of these measurements is not contingent on the use of any major components which are not already on hand or under construction, there will be some delays in

*Funding from this contract covered only a small part of the total project activity. The bulk of the funds provided for in this contract were utilized for certain crucial purposes as discussed later.

getting them to work as an integrated system. Present estimates are for data taking in early fall, say October.

(C) Other Relevant Information

1. Both the writing of this report and the seeking of new funding were delayed until solid evidence of progress and the system's overall feasibility could be presented. The results outlined in paragraph A(1) (discussed in more detail later) fulfill this immediate objective and a proposal has recently been submitted to the National Science Foundation for a grant totalling \$186,810 for a three year period.

2. The scope of the project has been enlarged by an on-going analytical study to determine the feasibility of measuring the viscosity of high temperature gases as well as their thermal conductivity.

3. Based upon the previous results of A. C. Chu in his 1970 Ph.D. dissertation, no difficulties of principle are foreseen once all the equipment is properly functioning. In anticipation of this development, preliminary initiatives are being taken to arrange the participation of another senior staff member on a visiting professorship basis.

4. The only permanent equipment request in the previously mentioned NSF proposal is for a high speed analog to digital data acquisition system, totaling \$27, 370. While it is possible to reduce data by the eye-hand-punch

card method from photographs of oscilloscope traces, this approach is both inaccurate and very time consuming. If we are successful in acquiring such a system, a very high level of productivity may be anticipated, hopefully justifying the years of tedious development work.

II. TECHNICAL DISCUSSION

The University of Wisconsin shock tube has been under continuous development since its adaptation to a combustion driver mode began in 1970 with the move to its present location in the Engineering Research Building. While it is possible to note some of the specific purposes for which Army funding was used, it is not possible to isolate particular results of the contract period due to this funding.

An overall summary of progress and the present state of the project will be given. More detailed accounts and technical developments are given in the MS thesis of F. P. Champomier (1972) and K. Chung (completion date: August, 1974).

(A) Summary of Novel Design Features and the Tube's Operation

Figures (1, 2, and 3) show overall views of the shock tube laboratory. Figure (3) shows the writer standing in front of the concrete anchor block in the driver room with the driver chamber retracted. Figure (4) shows a cross

section of the driver chamber and the transition to the shock duct embedded in the anchor block. The sizable recoil force of the driver chamber (up to 200 tons) is transmitted directly to the anchor block with twelve 1-3/8 in. dia. "redi-rods". Pre-stressing of the rods within the anchor block limits the elongation strain in the rods to the short distance between the left face of the anchor block and the flange of the driver chamber as shown in Figure (4). As a result, the joint containing the diaphragm between the driver chamber and the transition section is always under compression and is leak free.

The tightening and untightening of the large coupling nuts is easily done with an air impact wrench mounted on the outside of the driver chamber; its counterbalance and roller mounts permit easy access to all the nuts.

Once the diaphragm, the flexible linear shaped charge (FLSC), and its detonator are in place and the nuts tightened, the air in the chamber is pumped out and filling with the charge gases begins. The charge gases (75% of He and A mixture, 16 2/3% of H_2 and 8 1/3% O_2) are admitted to a separate mixing tank which contains a small fan to promote rapid mixing. Three mixing tank charges are needed to bring the driver chamber to its precombustion pressure of 255 psia.

All gas metering, mixing tank filling and discharge operations are controlled with solenoid or motor operated

valves remotely activated from the control console in the main laboratory area. When the ignition "arm" button is pushed, the chamber fill and gage lines are automatically isolated and purged with air so that if the explosion should get into these lines it would be incapable of further self-propagation.

Upon pushing the fire button, sparks are produced in three electrically shielded spark plugs which are located in the back wall of the driver chamber. The spark gaps are contained in the rear end of the ignition tubes which run the length of the chamber close to the inside walls. Thus the explosion pressure rise is initially confined to the tubes. However, very small ports distributed along the length of the tubes with several orientations produce a pattern of flame jets which criss cross the chamber.

As far as the writer knows the ignition design is original; it was designed to meet two objectives: (1) To promote a very rapid and turbulent combustion so as to smooth out Hopkinson effect non-uniformities with mixing. (2) To provide a uniform post combustion mixture in a state of thermodynamic equilibrium.

As later discussion will show it fulfills the objectives extremely well and has operated in this manner reliably for almost a year. However prior to this time great difficulties were encountered in learning how to avoid a

very violent detonative mode of combustion which rendered orderly shock propagation impossible; a year was lost in solving this problem. Figure (5) shows pressure time traces of the detonative and deflagration modes of combustion.

At a pre-set time after spark-ignition, the FLSC detonation frees the diaphragm and the high temperature and pressure combustion gases fulfill their function by driving a shock down the shock tube duct. The diaphragm rupture is timed to occur shortly after the peak pressure as shown in Figure (5c).

The combination of our very effective combustion system with this controlled rupture technique is at the heart of the performance success of our installation. Heretofore, the standard practice in most laboratories has been to let the combustion pressure rise stress the diaphragm beyond the yield point along carefully milled grooves. As the rupture pressure is not closely controllable, not only is the effective driver pressure rather unpredictable, but the gas driving the shock is still reacting and in a non-uniform state. This results in both somewhat unpredictable shock speeds and non-uniform post shock states. Our method avoids these effects. The use of FLSC for this purpose was suggested by Mr. Walter Dahl of the Rock Island Arsenal. Since we began to use it, the writer has indirectly heard of a Naval

installation which uses it, but the technique is still a largely a novel one.

After the FLSC frees the diaphragm, the 1500 psi pressure differential across the 0.039 in. thick diaphragm causes it to accelerate very rapidly indeed. It is prevented from being carried down the tube by folding around the upstream edge of a retaining plate which extends across the diameter of the transition section. If the extremely large kinetic energy of the folding motion is not dissipated, the diaphragm halves bounce from the side of the retainer plate and shread themselves in the high velocity gas. The shreaded high velocity diaphragm pieces pose a serious threat to the expensive windows, aerodynamic surfaces, etc. and constitute an intolerable risk.

After considerable effort over many months a fool-proof design of the retainer plate has been perfected. A pattern of knife edges and grooves cause the diaphragm halves to dissipate their energy in cutting and deforming themselves upon hitting the sides of the retainer plate; they remain tightly embedded on the first impact. Figure (6) illustrates the various stages of diaphragm use; the last picture of a ruptured diaphragm shows the general result but was made with an earlier retainer plate which did not have the knife edge feature. However, along with success in developing a trouble free mechanical design, metallurgical problems have arisen. Only a very hard tool steel,

Rockwell 46C or more, can retain the needed sharpness, but at the same time is also subject to cracking failure after 15 to 20 otherwise perfect shots. At present a retainer plate of type 430 Martensitic stainless steel is being made which can be heat treated to Rockwell 50C. The problem will be resolved.

Prior to firing, the shock tube duct and dump tank are evacuated to about 10^{-2} torr and the test gas is admitted. Its pressure is determined by the desired shock state, but typically it is in the range of 10 to 40 torr. Safety interlocks prevent firing until all pumps, gages, etc., are isolated from the high shock pressure surges. A special set of safety controls prevent test gas from being admitted directly to the vacuum pump (to prevent an explosion in the pump if the test gas is O_2).

Upon firing, a loud metallic bang is heard and floor vibrations can be sensed. Before jacks were installed to the ceiling, the dump tank [visible as the large tank in the foreground of Figure (1)] would lift off the floor by as much as 1/2 inch!

(B) Comparison of Theory and Experiment

Superscripts:

(*) a velocity or Mach number defined in laboratory coordinates.

(') a precombustion driver gas state.

Subscripts:

- 1 - pre-shock test gas state
- 2 - post shock test gas state
- 3 - expanded driver gas state
- 4 - initial, unexpanded driver gas state

1. A computer program for calculating the 2 state properties,

$$P_2, T_2, \rho_2, h_2, M_2, a_2 \text{ and } \alpha_2$$

as functions of

$$P_1, T_1 \text{ and } M_s^*$$

for real diatomic gases has been prepared. (a = acoustic velocity, α = degree of dissociation, M_s^* = shock Mach number). The program has been used to prepare a set of real gas shock tables. The results for $T_2 = T_2(M_s^*)$ in O_2 at a fixed T_1 and several P_1 values is shown in Figure (7). A similar curve for A from standard constant C_p shock tables is also included up to ionization temperatures.

2. A second computer program has been prepared for computing the following constant volume, post combustion, equilibrium state properties of the driver gas,

$$T_4, u_4, C_{p4}, a_4 \text{ and } \gamma_4$$

as a function of

$$P_4, \gamma_{He}$$

at the fixed values: $P_4' = 255$ psia, $T_4' = 297^\circ K$ and the composition, 75% inert, 16-2/3% H_2 and 8-1/3% O_2 (in which

$a_4 = \equiv \sqrt{(\partial P / \partial \rho)_s}$, $\gamma_4 \equiv (\partial \ln P / \partial \ln P)_s$ and $y_{He} =$
 $(He) / [(H_2) + (A)]$, the mol fraction of He in the inert
 component).

As the combustion is non-adiabatic the 4 state is
 variable, depending on the extent of heat transfer. In
 practice the program is entered with an experimental, trans-
 ducer measured P_4 value at the moment of diaphragm rupture,
 e.g., as from the Figure (5c) P_4 - time trace.

It should also be noted that, since on a per mol basis,
 the properties of He and A are identical, the relationship
 of T_4 , γ_4 and is unchanged by changes in y_{He} . On the other
 hand, those properties which depend on the molecular weight,
 especially a_4 , will vary with y_{He} . It is also of interest
 to observe that because of the 75% preponderance of inert
 components, the value of γ_4 is almost independent of P_4
 and T_4 as well as y_{He} .

3. If the standard equation for the isentropic, con-
 stant area, constant γ , unsteady expansion of a gas from
 an initial 4 state at rest to a moving 3 state if modified
 to allow for an area contraction prior to the sonic velocity
 plane there results

$$C \frac{P_3}{P_2} = \left[1 - \frac{\gamma_4 - 1}{2} \frac{u_3^*}{a_4} \right]^{\frac{2\gamma_4}{\gamma_4 - 1}}$$

in which C is a geometrical constant, determined by the
 area contraction ratio. However, across the contract region

between the driven 2 gas and the expanded driver 3 gas, we have the matching conditions:

$$P_3 = P_2 \quad (2)$$

$$u_3^* = u_2^* = u_s^* - u_2 = u_s^*(1 - \rho_1/\rho_2) \quad (3)$$

By introducing these relations into Equation (1) there results,

$$C\left(\frac{P_2}{P_1}\right)\left(\frac{P_1}{P_4}\right) = \left[1 - \frac{\gamma_4 - 1}{2} \left(\frac{a_1}{a_4}\right) M_s^* (1 - \rho_1/\rho_2)\right]^{\frac{2\gamma_4}{\gamma_4 - 1}} \quad (4)$$

in which P_2/P_1 , ρ_1/ρ_2 , and M_s^* are coupled by the real gas shock relations so that there is only a unique value of M_s^* which will satisfy Equation (4) and the shock relations. Thus for a given 1 state gas, the only parameters by which M_s^* can be varied are P_4 , a_4 and γ_4 . Of these it is not practical to significantly vary γ_4 . At this point another novel feature of the Wisconsin technique becomes clear: by simply varying the proportion of He and A in the fixed 75% inert component in the reactant mixture, it is possible to vary a_4 . Therefore it is possible to continuously vary M_s^* over a wide range without changes in diaphragm thickness, FLSC strength, precombustion pressure or filling procedure. This approach is considerably simpler and more flexible than the usual one of controlling M_s^* by varying P_4 .

The same principle can and is being adapted to the compressed gas mode of driving the shock for the lower Mach number range.

4. Figure (8a) shows a plot of experimental P_4 data vs. y_{He} . The least square fitted line which has the equation,

$$P_4(\text{psia}) = 1605.5(1 - 0.056 y_{\text{He}}) \quad (5)$$

is seen to decrease slightly with increasing replacement of A with He. This is consistent with the larger heat transfer losses to be expected as a consequence of helium's higher thermal conductivity.

The smooth curve of Figure (8b) is a plot of the M_s^* solutions of the real shock relations and Equation (4) with P_4 specified by Equation (5). This curve therefore represents the pre-shot prediction of M_s^* as a function of y_{He} , P_1 and other fixed parameters. Superimposed on the curve are experimental M_s^* values as measured from the timing of pressure transducer pulses at known locations in the shock tube test section. The resulting M_s^* were corroborated, within the accuracy of measurement, by the oscilloscope recorded pressure rises. The agreement between the experimental and calculated results is seen to be excellent, i.e., to better than $\pm 2\%$ as stated in the summary on page 1.

Another quantity of interest is the purely aerodynamic frictional loss. The effect of uncertainty in predicting P_4 can be eliminated by comparing the experimental M_s^* values with the ideal values computed from the individual measured P_4 values instead of the mean line value as in

Figure (8). Figure (9) shows that the slope of the M_S^* (experimental) vs. M_S^* (calculated) line is 0.99, i.e., aerodynamic losses cause the measured M_S^* to be 1% less than the ideal. This very encouraging result suggests that the high temperature test gas slug will be exceptionally "clean", i.e., free of extraneous disturbances.

(C) Range of Accessible Mach Numbers

Figure (10) shows the range of accessible Mach numbers with O_2 as a test gas at $P_1 = 20$ torr. Some variation in the relation of P_4 to M_S^* occurs as P_1 is varied but the results in Figure (10) are representative. The T_2 values corresponding to the M_S^* values are shown in Figure (7). Only the combustion mode with $0 \leq y_{He} \leq 1$ has yet been experimentally investigated in the present installation. Adaptations to the higher He and A supply pressure needed for the compressed gas mode are presently in progress. No difficulties are foreseen for this mode as it was used previously in Chu's dissertation work. At the high end of the M_S^* range, as one proceeds up the $y_{He} = 1$ curve the limit is set by the strength of the present 0.039 in thick diaphragms and is estimated to be at $P_4 = 2000$ psia giving an estimated maximum $M_S^* = 14.5$. Higher shock strengths are attainable with thicker diaphragms but this would entail heavier FLSC and considerable redesign.

III. IMMEDIATE AND LONG RANGE OBJECTIVES

(A) Complete the adaptation to the compressed gas mode to make the lower M_s^* range accessible.

(B) Complete the integration of the electronic and optical measurement systems.

(C) Carry out a limited thermal conductivity study in argon at sub-ionization temperatures. Both independent experimental data from the literature and reliable theory are available for A and it would be a good gas to "check out" the system on. The use of A as a test gas is the primary motivation for introducing the compressed gas mode of operation.

(D) Upon satisfactory completion of the A study, to begin an extensive study of O_2 .

(E) Carry out in parallel, if possible, measurements on CO which could be studied without high dissociation using the compressed gas mode.*

(F) Carry out an analytical study in parallel with the foregoing objectives to investigate the feasibility of measuring high temperature viscosity in the same general facility.

IV. CONTRIBUTION OF THE ARMY CONTRACT

While the dollar contribution of the Army contract was

*The concern at high dissociation is the state of agglomeration of the free carbon formed, $CO \rightarrow C_{(s)} + O$ etc.

small relative to the time integrated contributions of the NSF and other sources, it was received at a particularly crucial time when a funding was badly needed for certain major consumable supplies and for the construction of some large components which needed sizable block sums of money. These components are now an integral part of the installation and are in daily use. A rough unofficial list of these major expenses is given below.

- | | |
|--|----------|
| (1) The new test section, 6 ft. long,
all stainless steel - see Fig. (2) | |
| First payment: | \$ 9,000 |
| (2) Two fused silica windows, schlieren
grade, 14" x 5" x 1.5" | \$ 1,652 |
| (3) An ignition control system for
spark plugs and detonator with
adjustable time delay and several
safety interlocks | \$ 800 |
| (4) 150 ft. of flexible linear shaped
charge (FLSC) at 5gr/ft in plastic
holder. (The last of this purchase
is being used in the current week.) | \$ 433 |

Major expense total: \$11,884

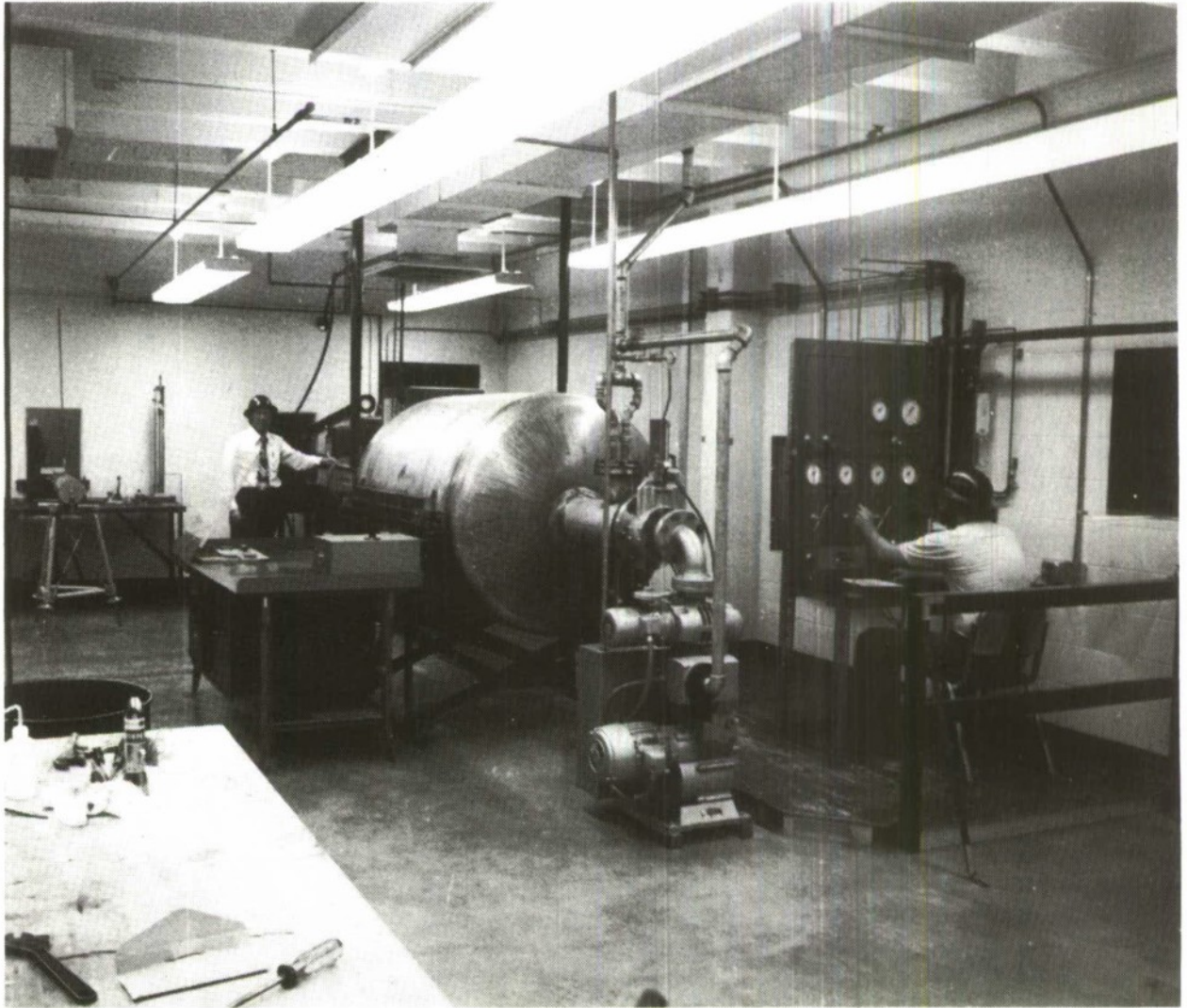


FIGURE (1) GENERAL VIEW OF THE SHOCK TUBE LABORATORY

The tube enters the laboratory from the driver room which is behind the writer in the center distance; the tube discharges into the large dump tank in the center. J. Wolske is at the control panel on the right. A small compressed helium shock tube for instrumentation testing is shown issuing from the driver room on the left.

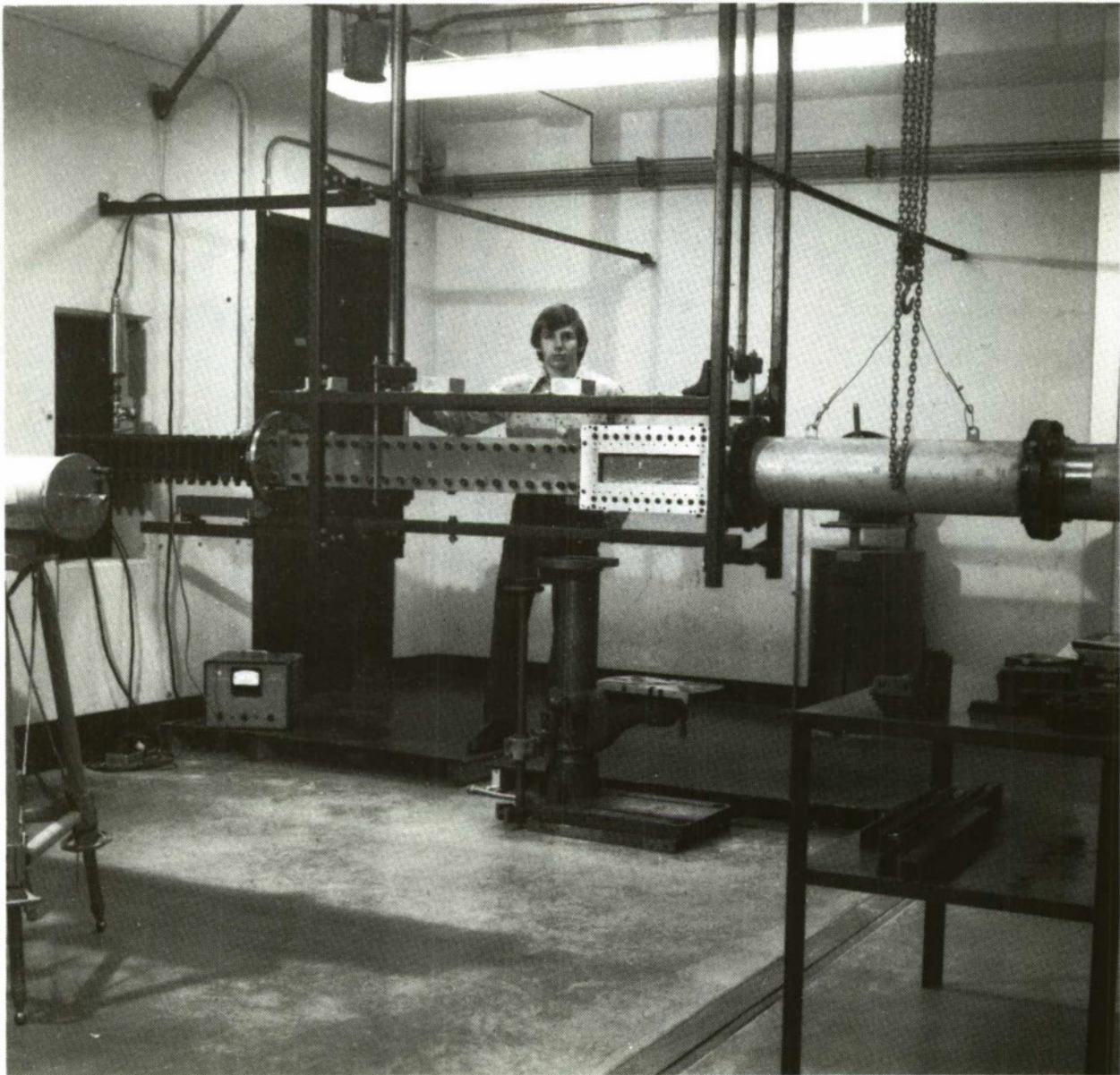


FIGURE (2) SHOCK TUBE TEST SECTION

The shock duct issues through the opening from the driver room at the left. The new, all stainless steel test section to which it connects is suspended from the ceiling. This provides clearance for the three channel photoelectric schlieren system which, when completed, will be supported by the old drill press mount shown. The window spaces are filled with metal blanks which will be replaced for testing the optical systems. The Unistrut frame surrounding the test section supports the laser shock velocity measurement system. The frame is independently supported from the ceiling to eliminate interference from floor vibrations when the tube is fired.

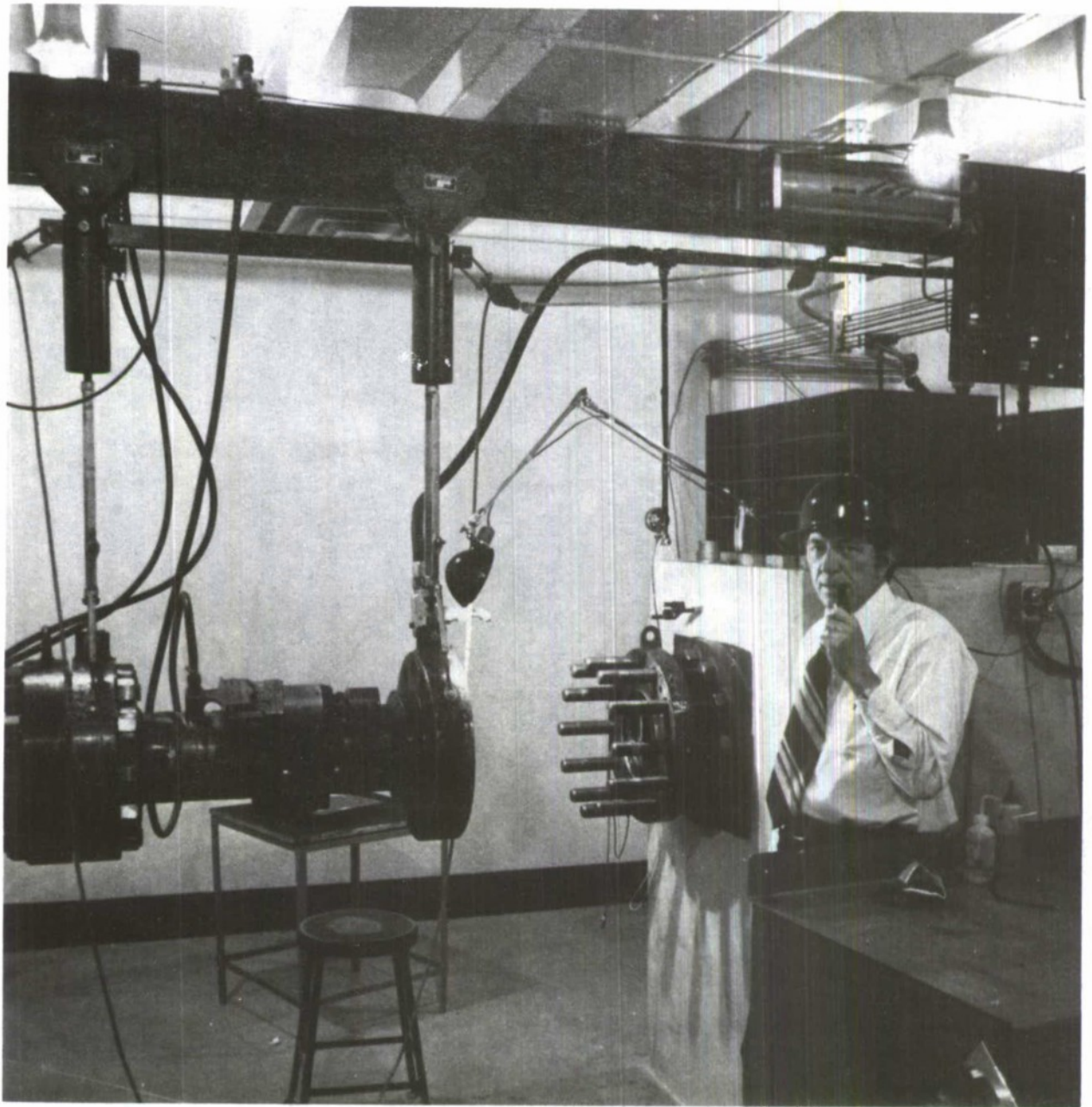


FIGURE (3) GENERAL VIEW IN THE DRIVER ROOM

The driver chamber, suspended from overhead rollers, couples to the shock duct entrance with a diaphragm between them. Tightening and untightening the nuts is done with the air impact wrench shown mounted on the driver chamber. As a short duration "kick" of up to 200 tons force may be generated by a shot, the large concrete anchor block behind the author serves to minimize the effects of vibration, stresses, etc. on the tube and instrumentation.

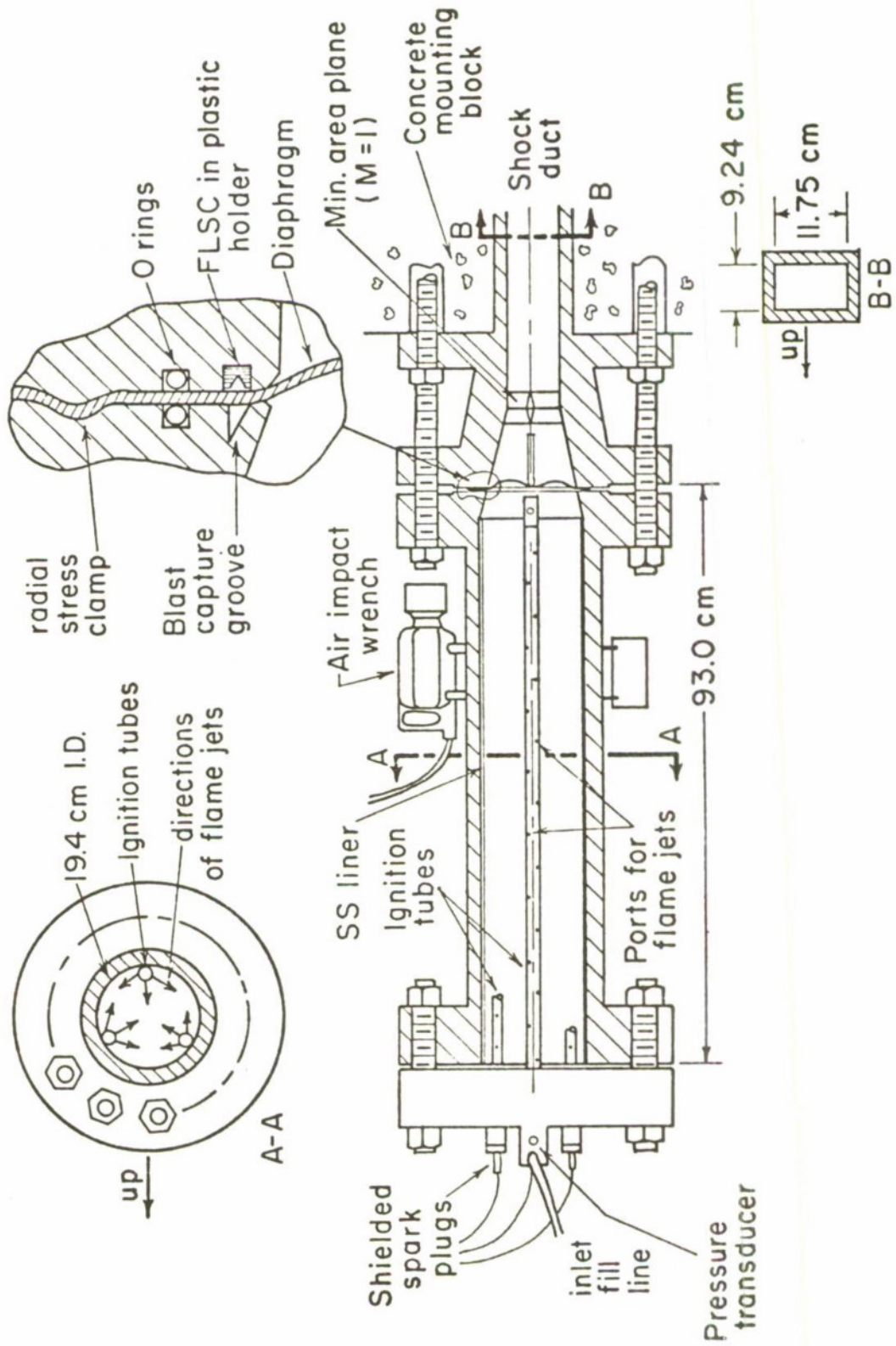
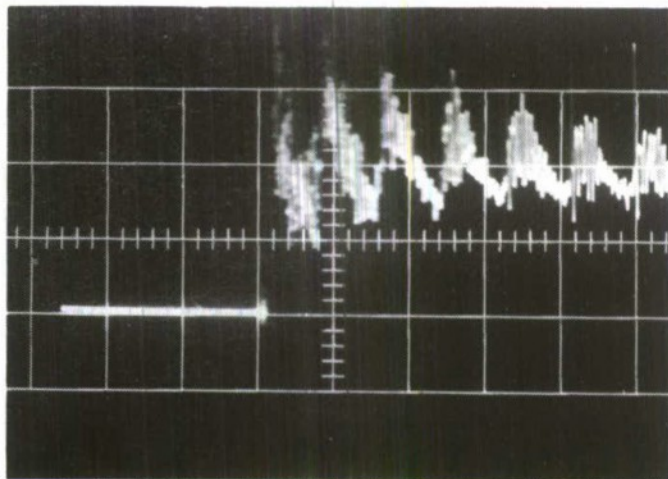


Fig.4 Plan view cross section of driver chamber and transition section.

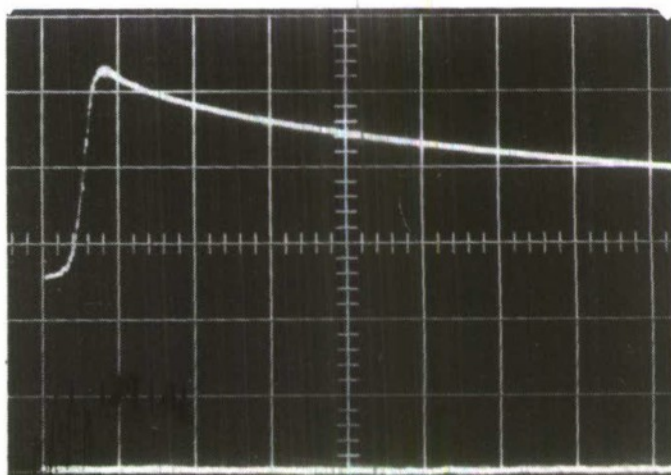
(a) Detonation mode of combustion with a blind flange in place of the diaphragm.

y axis, 530 psi/cm
x axis, 2ms/cm



(b) Deflagration mode of combustion with a blind flange in place of a diaphragm.

y axis, 530 psi/cm
x axis, 50 ms/cm



(c) Deflagration mode of combustion with shaped charge diaphragm cutting at a pre-set 76 ms. interval after ignition.

y axis, 530 psi/cm
x axis, 20 ms/cm

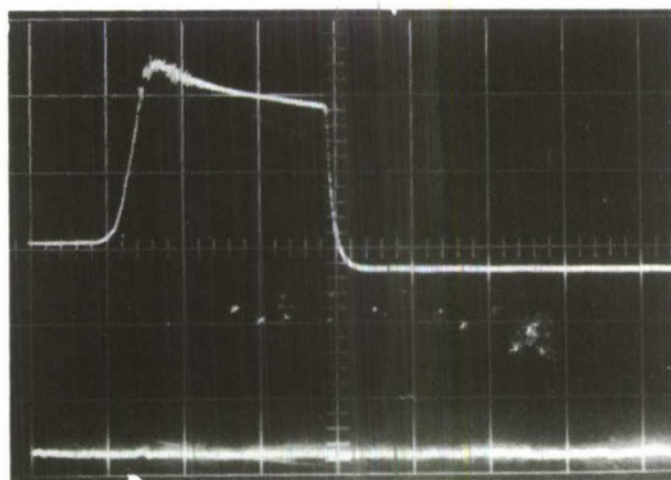


FIGURE (5) Pressure-time traces of H_2O_2 -He explosions in the driver chamber.

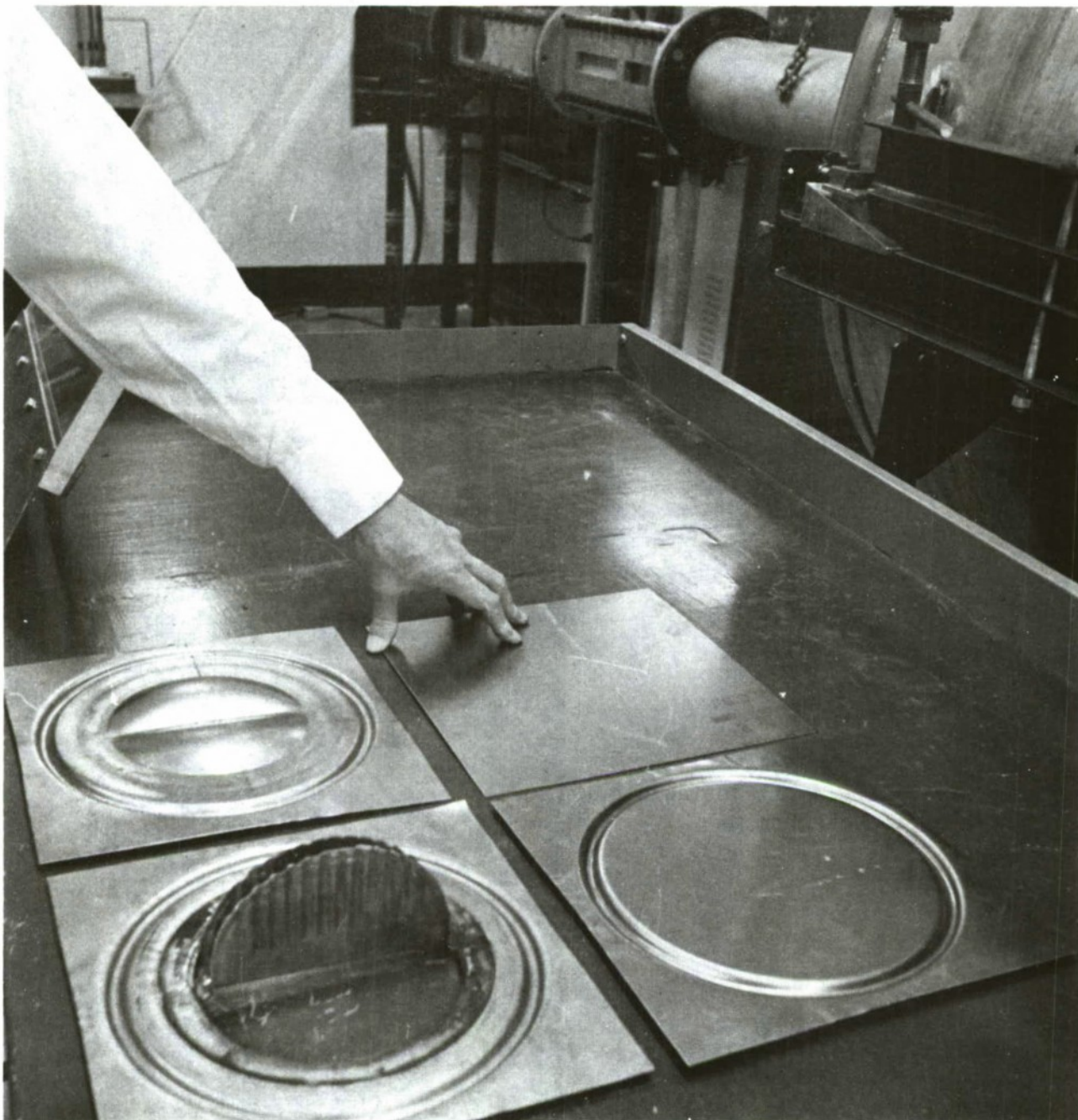


FIGURE (6) STAGES OF DIAPHRAGM USE

“Deep drawn killed quality” steel plate, 0.039 inches thick is used (top). Retaining grooves have been pressed into the plate (right). After the diaphragm contains the explosion without rupture it is left in the shape shown (left). After the driver gas has been released by shaped charge cutting of the diaphragm, it has the appearance above (bottom). The very large kinetic energy of the folding “petals” is dissipated by inelastic deformation of the petals against the grooves on the center plate.

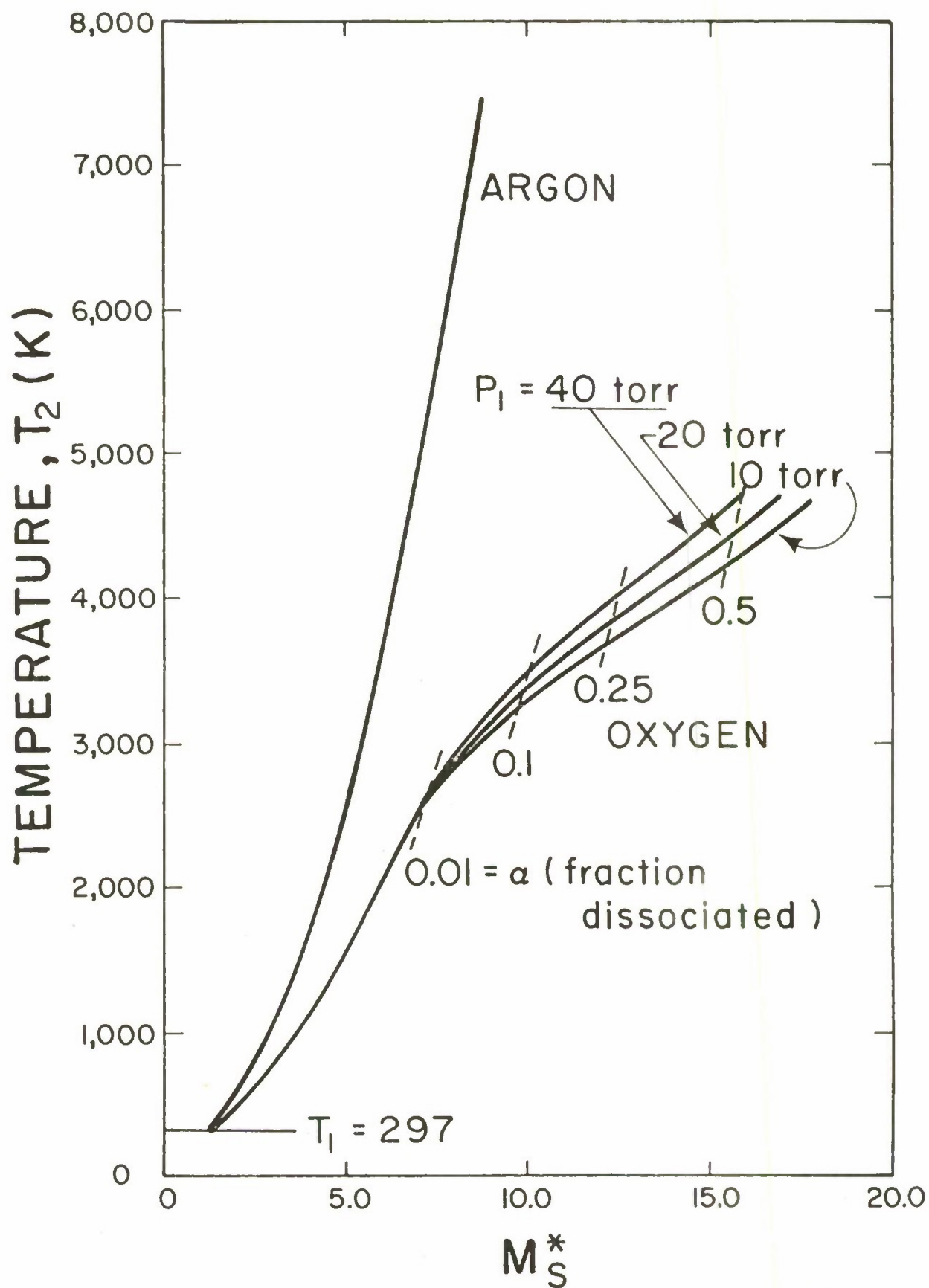


FIG. 7

T_2 as a function of M_S^*

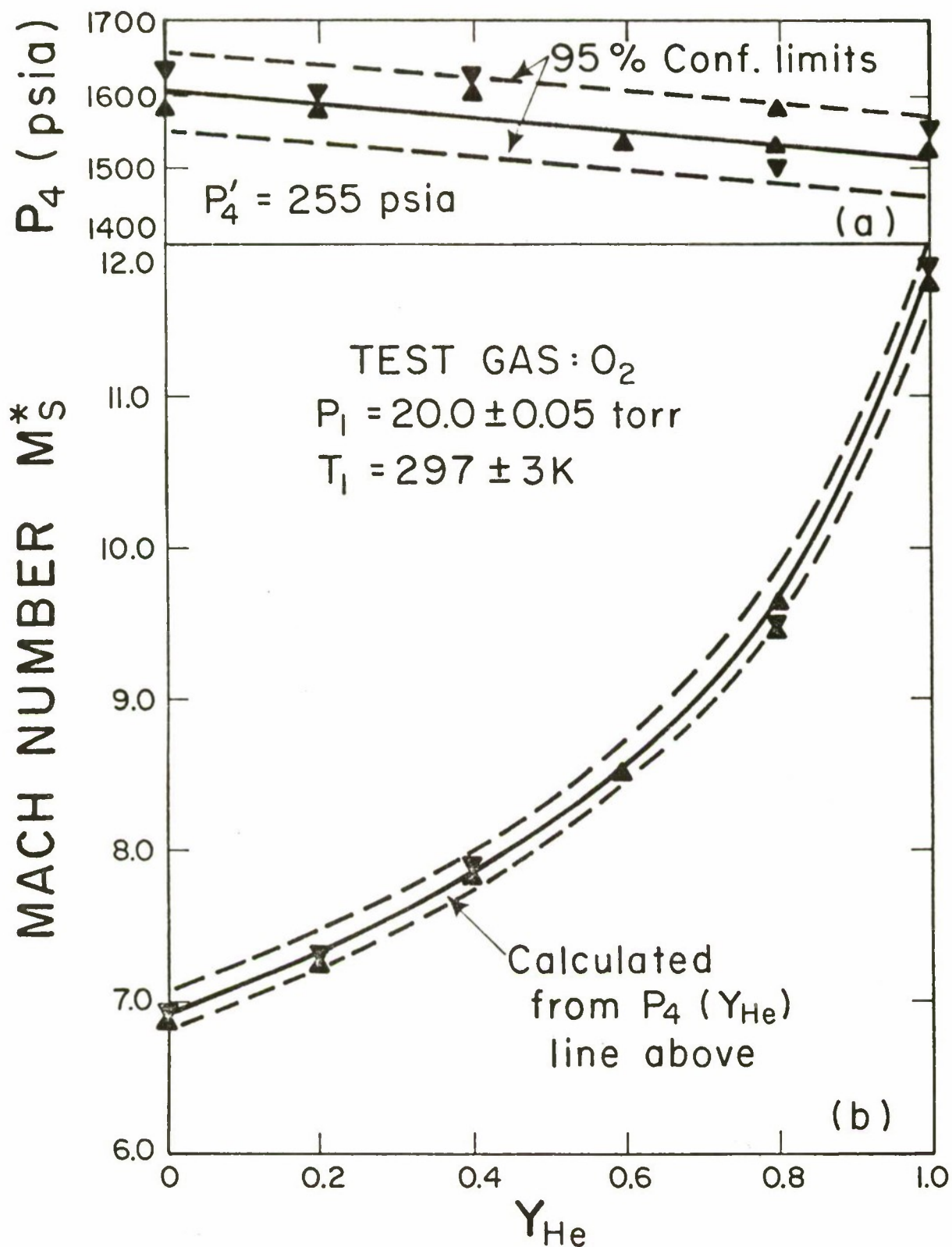


FIG. 8 Calculated and measured Mach numbers as functions of mol fraction He in Inert

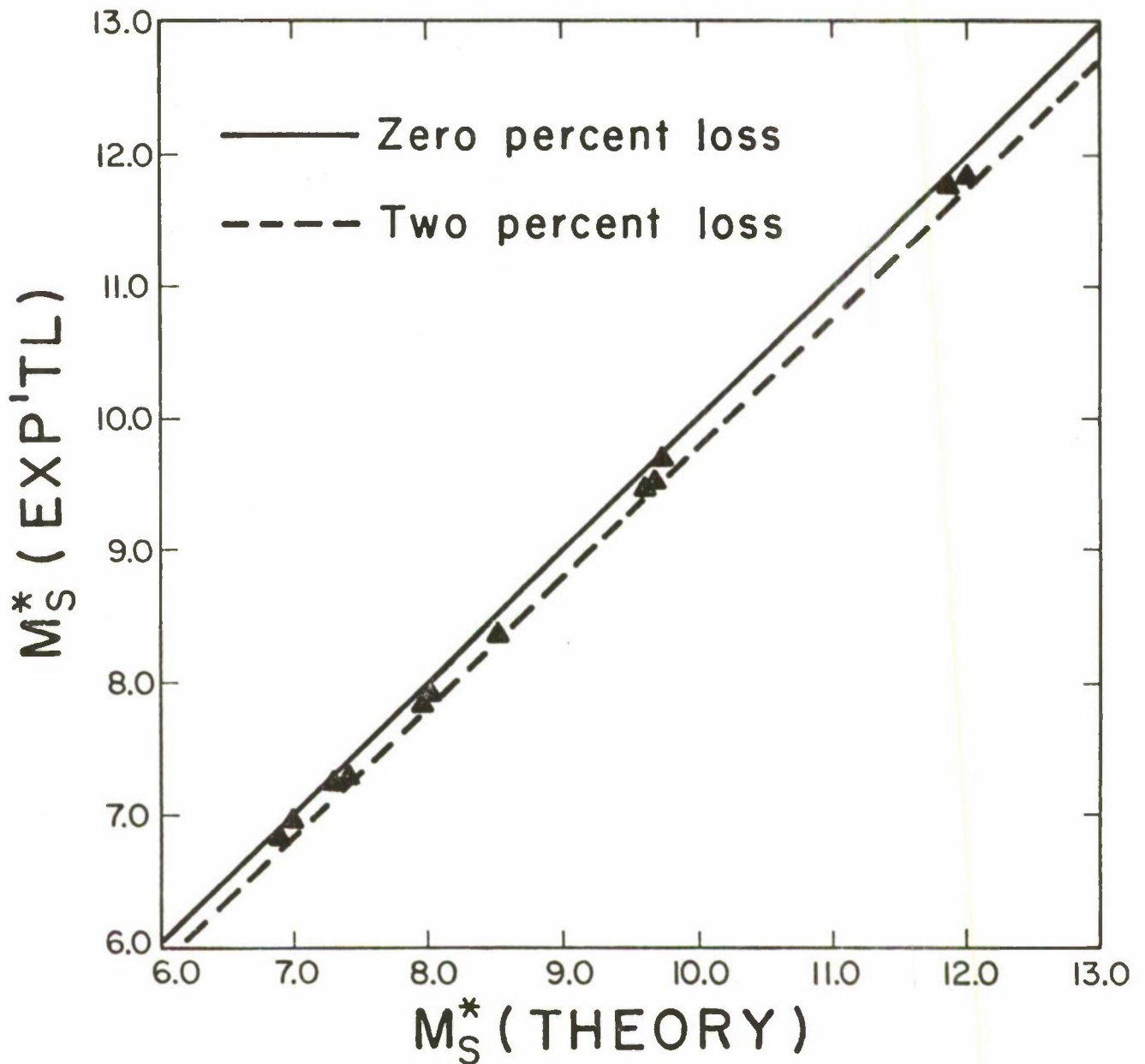


FIG. 9 Correlation of M_S^* (theory from individual P_4 measurement) with M_S^* (exp'tl) to show aerodynamic loss

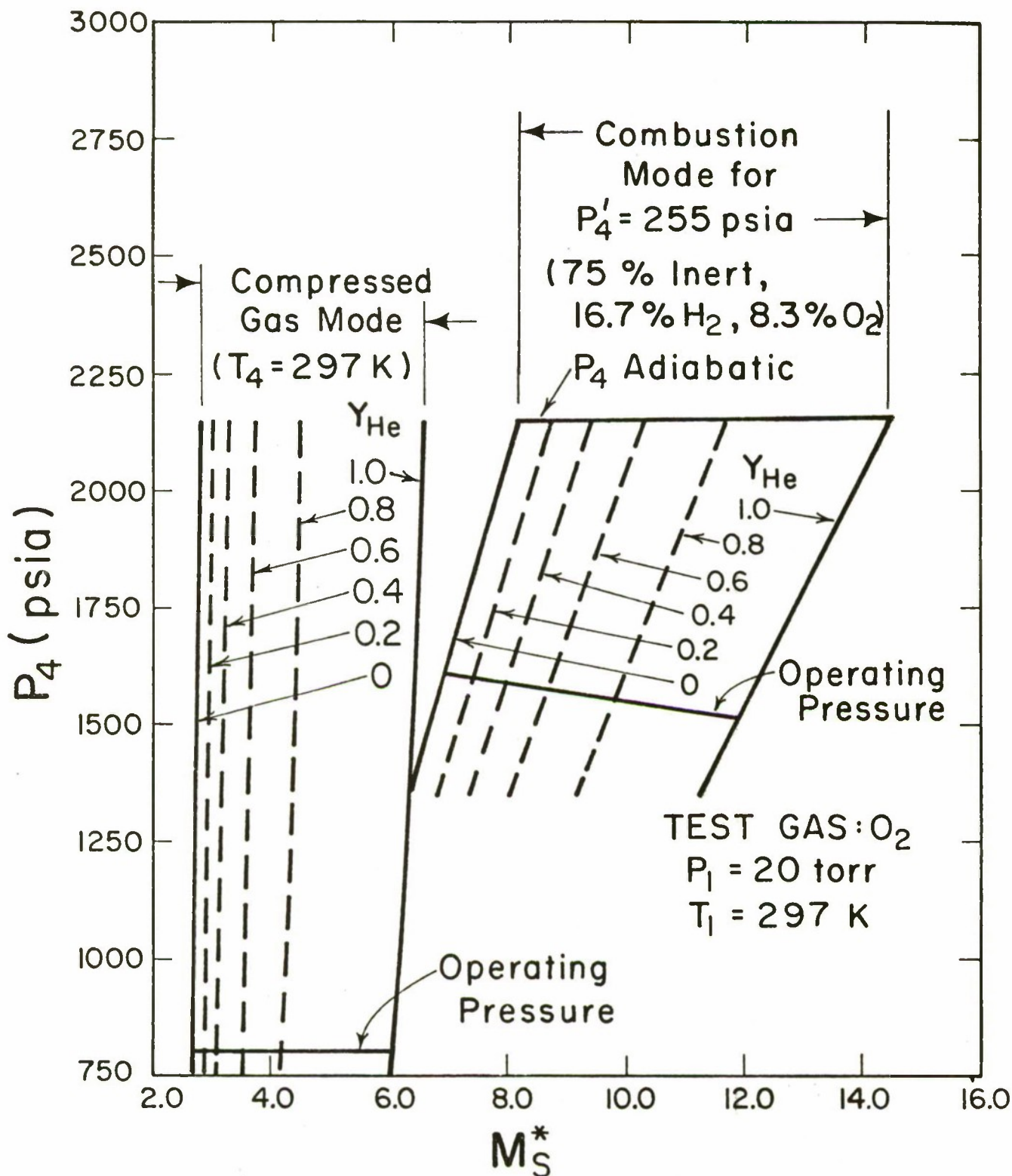


FIG. 10 Shock Mach number as a function of driver pressure, P_4 , and mol fraction He, Y_{He} in inert

DISTRIBUTION

Copies

A. Department of Defense

Office of the Director of Defense
Research & Engineering
ATTN: Mr. J. C. Barrett
Room 3D-1085, The Pentagon
Washington, DC 20301

1

Defense Documentation Center
ATTN: TIPDR
Cameron Station
Alexandria, VA 22314

12

B. Department of the Army

Commander
U. S. Army Materiel Development & Readiness Command
ATTN: DRCRD-TO
DRCRD-R, Mr. H. Cohen
5001 Eisenhower Avenue
Alexandria, VA 22333

1

1

Commander
U. S. Army Armament Command
ATTN: DRSAR-RDP
DRSAR-PP
DRSAR-PPI
DRSAR-TDC
Rock Island, IL 61201

1

1

1

2

Commander
U. S. Army Electronics Command
ATTN: DRSEL-TL-ME
Fort Monmouth, NJ 07703

1

Commander
Rock Island Arsenal
ATTN: SARRI-LA
SARRI-LE
SARRI-LS
SARRI-LW
SARRI-LPL
SARRI-LR
SARRI-LT
Rock Island, IL 61201

1

1

1

1

1

2

20

1

Commander
U. S. Army Missile Command
ATTN: DRSMI-RP
DRSMD-RRS Mr. R. E. Ely
DRSMI-RSM Mr. Whellahan
Redstone Arsenal, AL 35809

2

1

1

DISTRIBUTION

Copies

Commander U. S. Army MERDC ATTN: STSFB-GL Fort Belvoir, VA 22060	1
Commander U. S. Army Environmental Hygiene Agency Edgewood Arsenal, MD 21010	1
Commander U. S. Army Medical Biomechanical Research Laboratory ATTN: Library Fort Detrick Bldg. 568 Frederick, MD 21701	1
Commander Natick Laboratories Natick, MA 01760	1
Commander U. S. Army Aviation School ATTN: Office of the Librarian Fort Rucker, AL 36362	1
Director Joint Military Packaging Training Center ATTN: AMXPT-PT Aberdeen Proving Ground, MD 21005	1
Commander U. S. Army Tropic Test Center ATTN: STETC-MO-A Technical Library Drawer 942 Fort Clayton, Canal Zone 09827	1
Commander Tobyhanna Army Depot ATTN: AMC Packaging, Storage & Containerization Center Tobyhanna, PA 18466	1
Commander U. S. Army Production Equipment Agency Rock Island Arsenal Rock Island, IL 61201	2

DISTRIBUTION

	<u>Copies</u>
Commander U. S. Army Tank-Automotive Command ATTN: DRSTA -RPL Technical Library	1
DRSTA-RK Materials Laboratory	1
Warren, MI 48090	
 U. S. Army Research & Development Group (Europe) ATTN: Chief, Chemistry Branch FPO New York 09510	 1
 Commander U. S. Army Research Office P. O. Box 12211 Research Triangle Park, NC 27709	 1
 Commander Army Materials and Mechanics Research Center ATTN: AMXMR-PL Watertown, MA 02172	 1
 Commander Frankford Arsenal ATTN: SARFA-L1000	 1
SARFA-C2500	1
Philadelphia, PA 19137	
 Commander Picatinny Arsenal ATTN: Plastics & Packaging Lab	 1
PLASTEC	1
Dover, NJ 07801	
 Commander Edgewood Arsenal ATTN: SAREA-CL-A Edgewood, MD 21010	 1
 Commander Watervliet Arsenal ATTN: SARWV-RDR	 1
SARWV-RDT Library	1
Watervliet, NY 12189	

DISTRIBUTION

Copies

C. Department of Navy

Office of Naval Research

ATTN: ONR-471

Room 928, Ballston Tower No. 1

Arlington, VA 22217

1

Commander

Naval Sea Systems Command

ATTN: SEA-03

ATTN: RMA-54

ATTN: SP-271

Washington, DC 20362

1

1

1

Commander

Naval Supply Systems Command

ATTN: NSUP-048

Washington, DC 20376

1

Commander

U. S. Naval Surface Weapons Center

ATTN: NDL-211

Silver Springs, MD 20910

1

Commander

U. S. Naval Research Laboratory

ATTN: NRL-2600

Washington, DC 20375

1

Commander

U. S. Naval Ordnance Test Station

ATTN: Code 753 Technical Library

China Lake, CA 93555

1

Commander

Mare Island Naval Shipyard

ATTN: Rubber Laboratory

Vallejo, CA 94592

1

DISTRIBUTION

	<u>Copies</u>
D. <u>Department of the Air Force</u>	
HQ USAF RDP Room 4D-313, The Pentagon Washington, DC 20330	1
AFML/LTM Wright-Patterson AFB, OH 45433	2
AFML/MB Wright-Patterson AFB, OH 45433	1
AFFTC Edwards AFB, CA 93523	1
E. <u>Other Government Agencies</u>	
Energy Research and Development Agency Division of Reactor Development and Technology Washington, DC 20545	1
George C. Marshall Space Flight Center, NASA ATTN: M-S&E M-A&PS Huntsville, AL 35812	1 1

DISTRIBUTION LIST UPDATE

- - - FOR YOUR CONVENIENCE - - -

Government regulations require the maintenance of up-to-date distribution lists for technical reports. This form is provided for your convenience to indicate necessary changes or corrections.

If a change in our mailing lists should be made, please check the appropriate boxes below. For changes or corrections, show old address *exactly* as it appeared on the mailing label. Fold on dotted lines, tape or staple the lower edge together, and mail.

☐ Remove Name From List

Old Address:

☐ Change or Correct Address

Corrected or New Address:

COMMENTS

Date: _____ Signature: _____

Technical Report #

FOLD HERE

Return Address:

POSTAGE AND FEES PAID
DEPARTMENT OF THE ARMY
DOD 314



OFFICIAL BUSINESS
Penalty for Private Use \$300

Commander
Rock Island Arsenal
Attn: SARRI-LR
Rock Island, Illinois 61201

FOLD HERE

AD _____ ACCESSION NO. _____

Research Directorate
GEN Thomas J. Rodman Laboratory
Rock Island Arsenal, Rock Island, IL 61201
EXPERIMENTATION AND ANALYSIS TO PERFECT A
SHOCK PERTURBATION TECHNIQUE

Prepared by: Hugh N. Powell
Technical Report

26 pages, Incl Figures

The overall design of a shock tube has been validated with an extraordinary level of performance. It has been demonstrated that shock Mach numbers up to $M^*=12$ can be predicted to better than $\pm 2\%$ (95% confidence limits) and that the purely aerodynamic losses account for about a 1% decrease in the observed shock Mach numbers relative to the ideal performance values. These results set quite a new level of control for large high performance shock tube installations. The mechanical design work with complete reliability

(cont. over)

UNCLASSIFIED

1. Shock Tube Equipment
2. Construction
3. Operation
4. Thermal Conductivity

DISTRIBUTION

Approved for public release; Distribution Unlimited.

AD _____ ACCESSION NO. _____

Research Directorate
GEN Thomas J. Rodman Laboratory
Rock Island Arsenal, Rock Island, IL 61201
EXPERIMENTATION AND ANALYSIS TO PERFECT A
SHOCK PERTURBATION TECHNIQUE

Prepared by: Hugh N. Powell
Technical Report

26 pages, Incl Figures

The overall design of a shock tube has been validated with an extraordinary level of performance. It has been demonstrated that shock Mach numbers up to $M^*=12$ can be predicted to better than $\pm 2\%$ (95% confidence limits) and that the purely aerodynamic losses account for about a 1% decrease in the observed shock Mach numbers relative to the ideal performance values. These results set quite a new level of control for large high performance shock tube installations. The mechanical design work with complete reliability

(cont. over)

UNCLASSIFIED

1. Shock Tube Equipment
2. Construction
3. Operation
4. Thermal Conductivity

DISTRIBUTION

Approved for public release; Distribution Unlimited.

is demonstrated after extensive "de-bugging" the combustion, control and test section. The diaphragm rupture and folding system also functions with complete reliability with respect to diaphragm tearing, etc., but a presently unresolved problem is a material failure which occurs after 15 to 20 shots.

is demonstrated after extensive "de-bugging" the combustion, control and test section. The diaphragm rupture and folding system also functions with complete reliability with respect to diaphragm tearing, etc., but a presently unresolved problem is a material failure which occurs after 15 to 20 shots.